2009 American Control Conference
Hyatt Regency Riverfront, St. Louis, MO, USA
June 10-12, 2009

Decentralized Energy-Based Hybrid Control for the Multi-RTAC System

Jevon M. Avis, Sergey G. Nersesov, Rungun Nathan

Abstract— **The concept of decentralized energy-based hybrid control involves hybrid dynamic subcontrollers with discontinuous states that individually control each subsystem of a large interconnected dynamical system. Specifically, each subcontroller accumulates the emulated energy and when the states of the subcontroller coincide with a high emulated energy level, then we can reset these states to remove the emulated energy so that the emulated energy is not returned to the subsystem. The real physical energy of each subsystem in this case is constantly dissipated through the motion of the actuators due to the subcontroller state resettings. In this paper, we specialize the general decentralized energy-based hybrid control framework to interconnected Euler-Lagrange dynamical systems and experimentally verify it on the multi-RTAC (rotational/translational proof-mass actuator) system. In addition, we discuss hardware used and experimental testbed involving three RTAC carts connected by the springs and present experimental results using decentralized energy-based hybrid controllers. This testbed presents a unique experimental platform for studying benchmark problems in decentralized nonlinear control design.**

I. Introduction

In the control-system design of complex large-scale dynamical systems it is often desirable to treat the overall system as a collection of interconnected subsystems. The behavior of the composite (i.e., large-scale) system can then be predicted from the behaviors of the individual subsystems and their interconnections. The need for decentralized control design of large-scale systems is a direct consequence of the physical size and complexity of the dynamical model. Due to the broad range of applications of large-scale interconnected systems including mechanical systems, fluid systems, electromechanical systems, electrical systems, combustion systems, structural vibration systems, biological systems, physiological systems, power systems, telecommunications systems, and economic systems, to cite but a few examples, decentralized control has received considerable attention in the literature [1], [2], [3], [4], [5], [6], [7]. Some of the decentralized control techniques based on *subsystem decomposition* were studied in [1], [2], [3], [7] with control design procedures applied to the individual subsystems of the large-scale system.

Alternatively, a novel energy-based hybrid decentralized control framework for lossless and dissipative [8] large-scale dynamical systems based on subsystem decomposition was developed in [9]. The concept of an energy-based hybrid decentralized controller can be viewed as a feedback control technique that exploits the coupling between a physical large-scale dynamical system and an energy-based decentralized controller to efficiently remove energy from the physical large-scale system. Specifically, if a dissipative or lossless large-scale system is at high energy level, and a lossless feedback decentralized controller at a low energy level is attached to it, then subsystem energy will generally tend to flow from each subsystem into the corresponding subcontroller, decreasing the subsystem energy and increasing the subcontroller energy [10]. Of course, emulated energy, and not physical energy, is accumulated by each subcontroller. Conversely, if each attached subcontroller is at a high energy level and the corresponding subsystem is at a low energy level, then energy can flow from each subcontroller to each corresponding subsystem, since each subcontroller can generate real, physical energy to effect the required energy flow. Hence, if and when the subcontroller states coincide with a high emulated energy level, then we can *reset* these states to remove the emulated energy so that the emulated energy is not returned to the plant. This energy-dissipating hybrid control effectively enforces a one-way energy transfer between each subsystem and the corresponding subcontroller [11]. In this case, the overall closed-loop system consisting of the plant and the controller possesses discontinuous flows since it combines logical switchings with continuous dynamics, leading to impulsive differential equations [12], [13], [14].

In this paper, we specialize the decentralized energy-based hybrid control framework developed in [9] to interconnected Euler-Lagrange dynamical systems and experimentally apply it to stabilize the multi-RTAC system in real time. The RTAC system represents a translational oscillator and a rotational proof-mass attached to it. The nonlinear coupling between the rotational motion of the proof-mass and translational motion of the cart provides the basis for control. The problem of a single RTAC system stabilization has been extensively studied in the literature [15], [16], [17], [18] and presents a benchmark problem in nonlinear control design [19], [16], [20]. Furthermore, energy-based hybrid control for a single RTAC model was presented in [14] with its experimental validation shown in [21]. In this paper, we present the experimental testbed including three RTAC systems connected by springs for decentralized energy-based hybrid control design and discuss hardware implementation for this multi-RTAC system. This experimental testbed presents a unique testing platform which, in addition to traditional stabilization and tracking problems, allows for studying various physical phenomena such as Poincaré recurrence [22], [23], synchronization of mechanical systems [24], [25], [26], and chaos [27], to cite but a few examples.

II. Interconnected Euler-Lagrange Dynamical Systems

In this section, we specialize the decentralized energy-based hybrid control framework developed in [9] to interconnected Euler-Lagrange dynamical systems. For this, consider the governing equations of motion of an n-degree-of-freedom dynamical system given by the *Euler-Lagrange* equation

$$\frac{\mathrm{d}}{\mathrm{d}t}\left[\frac{\partial\mathcal{L}}{\partial\dot{q}}(q(t),\dot{q}(t))\right]^{\mathrm{T}}-\left[\frac{\partial\mathcal{L}}{\partial q}(q(t),\dot{q}(t))\right]^{\mathrm{T}} = u(t),$$

J.M. Avis and S.G. Nersesov are with the Department of Mechanical Engineering, Villanova University, Villanova, PA 19085-1681, USA (jevon.m.avis@villanova.edu; sergey.nersesov@villanova.edu).

R. Nathan is with the Division of Engineering, Pennsylvania State University, Reading, PA 19610, USA (rungun.nathan@psu.edu).

978-1-4244-4524-0/09/$25.00 ©2009 AACC

$$q(0) = q_0, \quad \dot{q}(0) = \dot{q}_0, \quad (1)$$

where $t \geq 0$, $q \in \mathbb{R}^n$ represents the generalized system positions, $\dot{q} \in \mathbb{R}^n$ represents the generalized system velocities, $\mathcal{L} : \mathbb{R}^n \times \mathbb{R}^n \to \mathbb{R}$ denotes the system Lagrangian given by $\mathcal{L}(q, \dot{q}) = T(q, \dot{q}) - U(q)$, where $T : \mathbb{R}^n \times \mathbb{R}^n \to \mathbb{R}$ is the system total kinetic energy and $U : \mathbb{R}^n \to \mathbb{R}$ is the system total potential energy, and $u \in \mathbb{R}^n$ is the vector of generalized control forces acting on the system. We assume that (1) represents an interconnected Euler-Lagrange dynamical system composed of s subsystems given by

$$\frac{\mathrm{d}}{\mathrm{d}t}\left[\frac{\partial \mathcal{L}}{\partial \dot{q}_i}(q(t), \dot{q}(t))\right]^{\mathrm{T}} - \left[\frac{\partial \mathcal{L}}{\partial q_i}(q(t), \dot{q}(t))\right]^{\mathrm{T}} = u_i(t), \quad i = 1, \ldots, s, \quad (2)$$

where $q_i \in \mathbb{R}^{n_i}$, $u_i \in \mathbb{R}^{n_i}$, $i = 1, \ldots, s$, $\sum_{i=1}^{s} n_i = n$, $q = [q_1^{\mathrm{T}}, \ldots, q_s^{\mathrm{T}}]^{\mathrm{T}}$, $u = [u_1^{\mathrm{T}}, \ldots u_s^{\mathrm{T}}]^{\mathrm{T}}$, q_i and $\dot{q}_i$ represent, respectively, generalized subsystem positions and velocities, and u_i denotes the vector of decentralized control input for the ith subsystem.

Furthermore, let $\mathcal{H} : \mathbb{R}^n \times \mathbb{R}^n \to \mathbb{R}$ denote the *Legendre transformation* of the Lagrangian function $\mathcal{L}(q, \dot{q})$ with respect to the generalized velocity $\dot{q}$ defined by $\mathcal{H}(q, p) \triangleq \dot{q}^{\mathrm{T}} p - \mathcal{L}(q, \dot{q})$, where p denotes the vector of generalized momenta given by $p(q, \dot{q}) = \left[\frac{\partial \mathcal{L}}{\partial \dot{q}}(q, \dot{q})\right]^{\mathrm{T}}$, and where the map from the generalized velocities $\dot{q}$ to the generalized momenta p is assumed to be *bijective* (i.e., one-to-one and onto). Note that $p = [p_1^{\mathrm{T}}, \ldots, p_s^{\mathrm{T}}]^{\mathrm{T}}$, where $p_i(q, \dot{q}) \triangleq \left[\frac{\partial \mathcal{L}}{\partial \dot{q}_i}(q, \dot{q})\right]^{\mathrm{T}}$, $i = 1, \ldots, s$, denotes the vector of the ith subsystem generalized momenta. We assume that the system total kinetic energy is such that $T(q, \dot{q}) = \frac{1}{2}\dot{q}^{\mathrm{T}}[\frac{\partial T}{\partial \dot{q}}(q, \dot{q})]^{\mathrm{T}}$, $T(q, 0) = 0$, and $T(q, \dot{q}) > 0$, $\dot{q} \neq 0$, $\dot{q} \in \mathbb{R}^n$. We also assume that the system total potential energy $U(\cdot)$ is such that $U(0) = 0$ and $U(q) > 0$, $q \neq 0$, $q \in \mathcal{D}_{\mathrm{q}} \subseteq \mathbb{R}^n$, which implies that $\mathcal{H}(q, p) = T(q, \dot{q}) + U(q) > 0$, $(q, \dot{q}) \neq 0$, $(q, \dot{q}) \in \mathcal{D}_{\mathrm{q}} \times \mathbb{R}^n$.

Next, we present a decentralized hybrid feedback control framework for Euler-Lagrange dynamical systems. Specifically, consider the ith subsystem (2) with output

$$y_i = \begin{bmatrix} h_{1i}(q_i) \\ h_{2i}(\dot{q}_i) \end{bmatrix} = \begin{bmatrix} h_{1i}(q_i) \\ h_{2i}\left(\frac{\partial \mathcal{H}}{\partial p_i}(q, p)\right) \end{bmatrix}, \quad (3)$$

where $i = 1, \ldots, s$, $y_i \in \mathbb{R}^{l_i}$, $h_{1i} : \mathbb{R}^{n_i} \to \mathbb{R}^{l_{1i}}$ and $h_{2i} : \mathbb{R}^{n_i} \to \mathbb{R}^{l_i - l_{1i}}$ are continuously differentiable, $h_{1i}(0) = 0$, $h_{2i}(0) = 0$, and $h_{1i}(q_i) \not\equiv 0$. Next, consider the decentralized energy-based hybrid controller for the ith subsystem

$$\frac{\mathrm{d}}{\mathrm{d}t}\left[\frac{\partial \mathcal{L}_{\mathrm{c}i}}{\partial \dot{q}_{\mathrm{c}i}}(q_{\mathrm{c}i}(t), \dot{q}_{\mathrm{c}i}(t), y_{q_i}(t))\right]^{\mathrm{T}} - \left[\frac{\partial \mathcal{L}_{\mathrm{c}i}}{\partial q_{\mathrm{c}i}}(q_{\mathrm{c}i}(t), \dot{q}_{\mathrm{c}i}(t), y_{q_i}(t))\right]^{\mathrm{T}} = 0,$$
$$q_{\mathrm{c}i}(0) = q_{\mathrm{c}i0}, \quad \dot{q}_{\mathrm{c}i}(0) = \dot{q}_{\mathrm{c}i0}, \quad (q_{\mathrm{c}i}(t), \dot{q}_{\mathrm{c}i}(t), y_i(t)) \notin \mathcal{Z}_{\mathrm{c}i}, \quad (4)$$

$$\begin{bmatrix} \Delta q_{\mathrm{c}i}(t) \\ \Delta \dot{q}_{\mathrm{c}i}(t) \end{bmatrix} = \begin{bmatrix} \eta_i(y_{q_i}(t)) - q_{\mathrm{c}i}(t) \\ -\dot{q}_{\mathrm{c}i}(t) \end{bmatrix}, \quad (q_{\mathrm{c}i}(t), \dot{q}_{\mathrm{c}i}(t), y_i(t)) \in \mathcal{Z}_{\mathrm{c}i}, \quad (5)$$

$$u_i(t) = \left[\frac{\partial \mathcal{L}_{\mathrm{c}i}}{\partial q_i}(q_{\mathrm{c}i}(t), \dot{q}_{\mathrm{c}i}(t), y_{q_i}(t))\right]^{\mathrm{T}}, \quad (6)$$

where $t \geq 0$, $i = 1, \ldots, s$, $q_{\mathrm{c}i} \in \mathbb{R}^{n_{\mathrm{c}i}}$ represents virtual subcontroller positions, $\dot{q}_{\mathrm{c}i} \in \mathbb{R}^{n_{\mathrm{c}i}}$ represents virtual subcontroller velocities, $n_{\mathrm{c}} \triangleq \sum_{i=1}^{s} n_{\mathrm{c}i}$, $y_{q_i} \triangleq h_{1i}(q_i)$, $\mathcal{L}_{\mathrm{c}i} : \mathbb{R}^{n_{\mathrm{c}i}} \times \mathbb{R}^{n_{\mathrm{c}i}} \times \mathbb{R}^{l_{1i}} \to \mathbb{R}$ denotes the subcontroller Lagrangian given by $\mathcal{L}_{\mathrm{c}i}(q_{\mathrm{c}i}, \dot{q}_{\mathrm{c}i}, y_{q_i}) \triangleq T_{\mathrm{c}i}(q_{\mathrm{c}i}, \dot{q}_{\mathrm{c}i}) - U_{\mathrm{c}i}(q_{\mathrm{c}i}, y_{q_i})$, where $T_{\mathrm{c}i} : \mathbb{R}^{n_{\mathrm{c}i}} \times \mathbb{R}^{n_{\mathrm{c}i}} \to \mathbb{R}$ is the subcontroller kinetic energy and $U_{\mathrm{c}i} : \mathbb{R}^{n_{\mathrm{c}i}} \times \mathbb{R}^{l_{1i}} \to \mathbb{R}$ is the subcontroller potential energy, $\eta_i(\cdot)$ is a continuously differentiable function such that $\eta_i(0) = 0$, $\mathcal{Z}_{\mathrm{c}i} \subset \mathbb{R}^{n_{\mathrm{c}i}} \times \mathbb{R}^{n_{\mathrm{c}i}} \times \mathbb{R}^{l_i}$ is the ith subcontroller resetting set, $\Delta q_{\mathrm{c}i}(t) \triangleq q_{\mathrm{c}i}(t^+) - q_{\mathrm{c}i}(t)$, $\Delta \dot{q}_{\mathrm{c}i}(t) \triangleq \dot{q}_{\mathrm{c}i}(t^+) - \dot{q}_{\mathrm{c}i}(t)$, and t_k, $k \in \overline{\mathbb{Z}}_+$, denotes a resetting instant. We assume that the subcontroller kinetic energy $T_{\mathrm{c}i}(q_{\mathrm{c}i}, \dot{q}_{\mathrm{c}i})$ is such that $T_{\mathrm{c}i}(q_{\mathrm{c}i}, \dot{q}_{\mathrm{c}i}) = \frac{1}{2}\dot{q}_{\mathrm{c}i}^{\mathrm{T}}[\frac{\partial T_{\mathrm{c}i}}{\partial \dot{q}_{\mathrm{c}i}}(q_{\mathrm{c}i}, \dot{q}_{\mathrm{c}i})]^{\mathrm{T}}$, with $T_{\mathrm{c}i}(q_{\mathrm{c}i}, 0) = 0$ and $T_{\mathrm{c}i}(q_{\mathrm{c}i}, \dot{q}_{\mathrm{c}i}) > 0$, $\dot{q}_{\mathrm{c}i} \neq 0$, $\dot{q}_{\mathrm{c}i} \in \mathbb{R}^{n_{\mathrm{c}i}}$. Furthermore, we assume that $U_{\mathrm{c}i}(\eta_i(y_{q_i}), y_{q_i}) = 0$ and $U_{\mathrm{c}i}(q_{\mathrm{c}i}, y_{q_i}) > 0$ for $q_{\mathrm{c}i} \neq \eta_i(y_{q_i})$, $q_{\mathrm{c}i} \in \mathbb{R}^{n_{\mathrm{c}i}}$.

We define the total energy of the interconnected system (1) as $V_{\mathrm{p}}(q, \dot{q}) \triangleq T(q, \dot{q}) + U(q)$ and we define the sum of subcontroller emulated energies as $V_{\mathrm{c}}(q_{\mathrm{c}}, \dot{q}_{\mathrm{c}}, y_q) \triangleq \sum_{i=1}^{s} T_{\mathrm{c}i}(q_{\mathrm{c}i}, \dot{q}_{\mathrm{c}i}) + U_{\mathrm{c}i}(q_{\mathrm{c}i}, y_{q_i}) = \sum_{i=1}^{s} V_{\mathrm{c}i}(q_{\mathrm{c}i}, \dot{q}_{\mathrm{c}i}, y_{q_i})$, where $q_{\mathrm{c}} \triangleq [q_{\mathrm{c}1}^{\mathrm{T}}, \ldots, q_{\mathrm{c}s}^{\mathrm{T}}]^{\mathrm{T}}$, $\dot{q}_{\mathrm{c}} \triangleq [\dot{q}_{\mathrm{c}1}^{\mathrm{T}}, \ldots, \dot{q}_{\mathrm{c}s}^{\mathrm{T}}]^{\mathrm{T}}$, and $y_q \triangleq [y_{q_1}^{\mathrm{T}}, \ldots, y_{q_s}^{\mathrm{T}}]^{\mathrm{T}}$. Finally, we define the total energy of the interconnected closed-loop system (2)–(6) as

$$V(q, \dot{q}, q_{\mathrm{c}}, \dot{q}_{\mathrm{c}}) \triangleq V_{\mathrm{p}}(q, \dot{q}) + V_{\mathrm{c}}(q_{\mathrm{c}}, \dot{q}_{\mathrm{c}}, y_q). \quad (7)$$

Next, we study the behavior of the total energy function $V(q, \dot{q}, q_{\mathrm{c}}, \dot{q}_{\mathrm{c}})$ along the trajectories of the closed-loop system dynamics. For the interconnected closed-loop system (2)–(6), we define the resetting set as

$$\mathcal{Z} \triangleq \cup_{i=1}^{s}\{(q, \dot{q}, q_{\mathrm{c}}, \dot{q}_{\mathrm{c}}) \in \mathcal{D}_{\mathrm{q}} \times \mathbb{R}^n \times \mathbb{R}^{n_{\mathrm{c}}} \times \mathbb{R}^{n_{\mathrm{c}}} : (q_{\mathrm{c}i}, \dot{q}_{\mathrm{c}i}, y_i) \in \mathcal{Z}_{\mathrm{c}i}\}. \quad (8)$$

Note that $\frac{\mathrm{d}}{\mathrm{d}t}V_{\mathrm{p}}(q, \dot{q}) = \frac{\mathrm{d}}{\mathrm{d}t}\mathcal{H}(q, p) = u^{\mathrm{T}}\dot{q}$, $(q, \dot{q}, q_{\mathrm{c}}, \dot{q}_{\mathrm{c}}) \notin \mathcal{Z}$. Furthermore, we define the ith subcontroller Hamiltonian by

$$\mathcal{H}_{\mathrm{c}i}(q_{\mathrm{c}i}, \dot{q}_{\mathrm{c}i}, p_{\mathrm{c}i}, y_{q_i}) \triangleq \dot{q}_{\mathrm{c}i}^{\mathrm{T}} p_{\mathrm{c}i} - \mathcal{L}_{\mathrm{c}i}(q_{\mathrm{c}i}, \dot{q}_{\mathrm{c}i}, y_{q_i}), \quad i = 1, \ldots, s, \quad (9)$$

where the subcontroller momentum $p_{\mathrm{c}i}$ is given by $p_{\mathrm{c}i}(q_{\mathrm{c}i}, \dot{q}_{\mathrm{c}i}, y_{q_i}) = \left[\frac{\partial \mathcal{L}_{\mathrm{c}i}}{\partial \dot{q}_{\mathrm{c}i}}(q_{\mathrm{c}i}, \dot{q}_{\mathrm{c}i}, y_{q_i})\right]^{\mathrm{T}}$, and it follows from the structure of $T_{\mathrm{c}i}(q_{\mathrm{c}i}, \dot{q}_{\mathrm{c}i})$ that $\mathcal{H}_{\mathrm{c}i}(q_{\mathrm{c}i}, \dot{q}_{\mathrm{c}i}, p_{\mathrm{c}i}, y_{q_i}) = V_{\mathrm{c}i}(q_{\mathrm{c}i}, \dot{q}_{\mathrm{c}i}, y_{q_i}) = T_{\mathrm{c}i}(q_{\mathrm{c}i}, \dot{q}_{\mathrm{c}i}) + U_{\mathrm{c}i}(q_{\mathrm{c}i}, y_{q_i})$. Now, it follows from (4), (6), and (9) that, for $t \in (t_k, t_{k+1}]$,

$$\frac{\mathrm{d}}{\mathrm{d}t}V_{\mathrm{c}i}(q_{\mathrm{c}i}(t), \dot{q}_{\mathrm{c}i}(t), y_{q_i}(t)) = -u_i^{\mathrm{T}}(t)\dot{q}_i(t), \quad (q(t), \dot{q}(t), q_{\mathrm{c}}(t), \dot{q}_{\mathrm{c}}(t)) \notin \mathcal{Z}. \quad (10)$$

Hence,

$$\frac{\mathrm{d}}{\mathrm{d}t}V(q(t), \dot{q}(t), q_{\mathrm{c}}(t), \dot{q}_{\mathrm{c}}(t)) = u(t)^{\mathrm{T}}\dot{q}(t) - \sum_{i=1}^{s} u_i^{\mathrm{T}}(t) q_i(t) = 0, \quad (q(t), \dot{q}(t), q_{\mathrm{c}}(t), \dot{q}_{\mathrm{c}}(t)) \notin \mathcal{Z}, \quad t_k < t \leq t_{k+1}, \quad (11)$$

which implies that the total energy of the interconnected closed-loop system between resetting events is conserved.

The total energy difference across resetting events can be shown to satisfy

$$\Delta V(q(t_k), \dot{q}(t_k), q_{\mathrm{c}}(t_k), \dot{q}_{\mathrm{c}}(t_k)) < 0, \quad (q(t_k), \dot{q}(t_k), q_{\mathrm{c}}(t_k), \dot{q}_{\mathrm{c}}(t_k)) \in \mathcal{Z}, \quad k \in \overline{\mathbb{Z}}_+. \quad (12)$$

In fact, the resetting law (5) ensures the total energy decrease across resetting events by an amount equal to the accumulated emulated subcontroller energy.

Here, we consider decentralized energy-dissipating state-dependent resetting controllers that affect a one-way energy transfer between the corresponding subsystem and the subcontroller. Specifically, consider the closed-loop system (2)–(6), where $\mathcal{Z}_{\mathrm{c}i}$, $i = 1, \ldots, s$, are defined by

$$\mathcal{Z}_{\mathrm{c}i} \triangleq \Big\{(q_i, \dot{q}_i, q_{\mathrm{c}i}, \dot{q}_{\mathrm{c}i}) : \frac{\mathrm{d}}{\mathrm{d}t}V_{\mathrm{c}i}(q_{\mathrm{c}i}, \dot{q}_{\mathrm{c}i}, y_{q_i}) = 0 \text{ and } V_{\mathrm{c}i}(q_{\mathrm{c}i}, \dot{q}_{\mathrm{c}i}, y_{q_i}) > 0\Big\}. \quad (13)$$

For practical implementation, knowledge of q_{c}, $\dot{q}_{\mathrm{c}}$, and y_q is sufficient to determine whether or not the closed-loop state vector is in the set $\mathcal{Z}$ given by (8), where $\mathcal{Z}_{\mathrm{c}i}$, $i = 1, \ldots, s$, are defined by (13).

The following definition is needed for the main result of this section. First, however, recall that the *Lie derivative* of a smooth function $\mathcal{X} : \mathcal{D} \to \mathbb{R}$ along the vector field of the continuous-time dynamics $f(x)$ is given by $L_f\mathcal{X}(x) \triangleq \frac{\mathrm{d}}{\mathrm{d}t}\mathcal{X}(\psi(t,x))|_{t=0} = \frac{\partial \mathcal{X}(x)}{\partial x} f(x)$, where $\psi(t,x)$, $t \geq 0$, is the solution to

$$\dot{x}(t) = f(x(t)), \quad x(0) = x_0, \quad t \geq 0, \quad (14)$$

with the initial condition $x_0 = x$, and the *zeroth* and *higher-order Lie derivatives* are, respectively, defined by $L_f^0\mathcal{X}(x) \triangleq \mathcal{X}(x)$ and $L_f^k\mathcal{X}(x) \triangleq L_f(L_f^{k-1}\mathcal{X}(x))$, where $k \geq 1$.

Definition 2.1: Let $\mathcal{M} \triangleq \cup_{i=1}^{q}\{x \in \mathcal{D} : \mathcal{X}_i(x) = 0\}$, where $\mathcal{X}_i : \mathcal{D} \to \mathbb{R}$, $i = 1, \ldots, q$, are infinitely differentiable functions. A point $x \in \mathcal{M}$ such that $f(x) \neq 0$ is *k-transversal* to (14) if there exist $k_i \in \{1, 2, \ldots\}$, $i = 1, \ldots, q$, such that

$$L_f^r\mathcal{X}_i(x) = 0, \quad r = 0, \ldots, 2k_i - 2, \quad L_f^{2k_i-1}\mathcal{X}_i(x) \neq 0, \quad i = 1, \ldots, q. \quad (15)$$

The next theorem gives sufficient conditions for stabilization of interconnected Euler-Lagrange dynamical systems using decentralized energy-based hybrid controllers. For this result define the closed-loop system states $x \triangleq [q^{\mathrm{T}}, \dot{q}^{\mathrm{T}}, q_{\mathrm{c}}^{\mathrm{T}}, \dot{q}_{\mathrm{c}}^{\mathrm{T}}]^{\mathrm{T}}$.

Theorem 2.1: Consider the interconnected closed-loop dynamical system $\mathcal{G}$ given by (2)–(6), with the resetting set $\mathcal{Z}$ given by (8), where $\mathcal{Z}_{\mathrm{c}i}$, $i = 1, \ldots, s$, are defined by (13). Assume that $\mathcal{D}_{\mathrm{c}i} \subset \mathcal{D}_{\mathrm{q}} \times \mathbb{R}^n \times \mathbb{R}^{n_{\mathrm{c}}} \times \mathbb{R}^{n_{\mathrm{c}}}$ is a compact positively invariant set with respect to $\mathcal{G}$ such that $0 \in \overset{\circ}{\mathcal{D}}_{\mathrm{c}i}$. Furthermore, assume that the k-transversality condition (15) holds for the continuous-time dynamics of the closed-loop system (2)–(6) with $\mathcal{X}_i(x) = \frac{\mathrm{d}}{\mathrm{d}t}V_{\mathrm{c}i}(q_{\mathrm{c}i}, \dot{q}_{\mathrm{c}i}, y_{q_i})$, $i = 1, \ldots, s$. Then the zero solution $x(t) \equiv 0$ to $\mathcal{G}$ is asymptotically stable. Finally, if $\mathcal{D}_{\mathrm{q}} = \mathbb{R}^n$ and the total energy function $V(x)$ is radially unbounded, then the zero solution $x(t) \equiv 0$ to $\mathcal{G}$ is globally asymptotically stable.

Proof. The proof is omitted due to page limitation. □

III. MULTI-RTAC SYSTEM

In this section, we describe the multi-RTAC nonlinear system and design decentralized energy-based hybrid controllers to stabilize the zero equilibrium state. The multi-RTAC system shown in Figure 1 consists of three identical translational oscillating carts connected by linear springs along with three identical eccentric rotational inertias which act as proof-mass actuators mounted on each cart. Rotational motion of each proof-mass is nonlinearly coupled with the translational motion of the corresponding cart that the proof-mass is mounted on which provides the mechanism for control. The oscillator carts, each with mass M, are connected to each other as well as fixed supports via linear springs of stiffness k. The carts are constrained to one-dimensional motion and the rotational proof-mass actuators consist of mass m and mass moment of inertia I located at a distance e from the axis of rotation.

Letting q_i and $\dot{q}_i$, $i = 1, 2, 3$, denote the translational position and velocity of each cart, letting θ_i and $\dot{\theta}_i$, $i = 1, 2, 3$, denote the angular position and angular velocity of each rotational proof-mass, and letting N_1, N_2, and N_3 denote the control torques applied to each proof-mass, we use the total physical energy of the multi-RTAC system

$$\begin{aligned} V_{\mathrm{p}}(q_i, \dot{q}_i, \theta_i, \dot{\theta}_i) \quad = \quad & k(q_1^2 + q_2^2 + q_3^2 - q_1q_2 - q_2q_3) \\ & + \frac{1}{2}(M + m)(\dot{q}_1^2 + \dot{q}_2^2 + \dot{q}_3^2) \\ & + \frac{1}{2}(I + me^2)(\dot{\theta}_1^2 + \dot{\theta}_2^2 + \dot{\theta}_3^2) \\ & + me(\dot{q}_1\dot{\theta}_1\cos\theta_1 + \dot{q}_2\dot{\theta}_2\cos\theta_2 \\ & + \dot{q}_3\dot{\theta}_3\cos\theta_3) \\ & + mge[(1 - \cos\theta_1) + (1 - \cos\theta_2) \\ & + (1 - \cos\theta_3)], \end{aligned} \quad (16)$$

to obtain the dynamic equations of motion given by

$$(M + m)\ddot{q}_1 = -me(\ddot{\theta}_1\cos\theta_1 - \dot{\theta}_1^2\sin\theta_1) - 2kq_1 + kq_2, \quad (17)$$

$$(I + me^2)\ddot{\theta}_1 = -me\ddot{q}_1\cos\theta_1 - mge\sin\theta_1 + N_1, \quad (18)$$

$$(M + m)\ddot{q}_2 = -me(\ddot{\theta}_2\cos\theta_2 - \dot{\theta}_2^2\sin\theta_2) + kq_1 - 2kq_2 + kq_3, \quad (19)$$

$$(I + me^2)\ddot{\theta}_2 = -me\ddot{q}_2\cos\theta_2 - mge\sin\theta_2 + N_2, \quad (20)$$

$$(M + m)\ddot{q}_3 = -me(\ddot{\theta}_3\cos\theta_3 - \dot{\theta}_3^2\sin\theta_3) + kq_2 - 2kq_3, \quad (21)$$

$$(I + me^2)\ddot{\theta}_3 = -me\ddot{q}_3\cos\theta_3 - mge\sin\theta_3 + N_3, \quad (22)$$

with the problem data given in Table I, decentralized control inputs $u_i = N_i$, $i = 1, 2, 3$, and outputs $y_i = \theta_i$, $i = 1, 2, 3$.

To design decentralized state-dependent hybrid controllers for (17)–(22), let $n_{\mathrm{c}i} = 1$, $V_{\mathrm{c}i}(q_{\mathrm{c}i}, \dot{q}_{\mathrm{c}i}, \theta_i) = \frac{1}{2}m_{\mathrm{c}}\dot{q}_{\mathrm{c}i}^2 + \frac{1}{2}k_{\mathrm{c}}(q_{\mathrm{c}i} - \theta_i)^2$, $\mathcal{L}_{\mathrm{c}i}(q_{\mathrm{c}i}, \dot{q}_{\mathrm{c}i}, \theta_i) = \frac{1}{2}m_{\mathrm{c}}\dot{q}_{\mathrm{c}i}^2 - \frac{1}{2}k_{\mathrm{c}}(q_{\mathrm{c}i} - \theta_i)^2$, $y_{qi} = \theta_i$, and $\eta_i(y_{qi}) = y_{qi}$, where $m_{\mathrm{c}} > 0$ and $k_{\mathrm{c}} > 0$, and $i = 1, 2, 3$. Then decentralized state-dependent hybrid subcontroller has the form

$$m_{\mathrm{c}}\ddot{q}_{\mathrm{c}i} + k_{\mathrm{c}}(q_{\mathrm{c}i} - \theta_i) = 0, \quad (q_{\mathrm{c}i}, \dot{q}_{\mathrm{c}i}, \theta_i, \dot{\theta}_i) \notin \mathcal{Z}_i, \quad (23)$$

$$\begin{bmatrix} \Delta q_{\mathrm{c}i} \\ \Delta \dot{q}_{\mathrm{c}i} \end{bmatrix} = \begin{bmatrix} \theta_i - q_{\mathrm{c}i} \\ -\dot{q}_{\mathrm{c}i} \end{bmatrix}, \quad (q_{\mathrm{c}i}, \dot{q}_{\mathrm{c}i}, \theta_i, \dot{\theta}_i) \in \mathcal{Z}_i, \quad (24)$$

$$u_i = k_{\mathrm{c}}(q_{\mathrm{c}i} - \theta_i), \quad (25)$$

with the resetting set (13) taking the form

$$\mathcal{Z}_i = \Big\{(q_{\mathrm{c}i}, \dot{q}_{\mathrm{c}i}, \theta_i, \dot{\theta}_i) \in \mathbb{R}^4 : k_{\mathrm{c}}\dot{\theta}_i(q_{\mathrm{c}i} - \theta_i) = 0 \text{ and } \begin{bmatrix} \theta_i - q_{\mathrm{c}i} \\ -\dot{q}_{\mathrm{c}i} \end{bmatrix} \neq 0\Big\}. \quad (26)$$

It was shown in [14] that the closed-loop system (17)–(22) and (23)–(26) satisfies k-transversality condition given in Definition 2.1, and hence, by Theorem 2.1, is globally asymptotically stable. In the next section, we implement the decentralized energy-based hybrid control framework on the multi-RTAC testbed and present the experimental results.

Description	Parameter	Value	Units
Cart mass	M	1.7428	kg
Eccentric mass	m	0.2739	kg
Arm eccentricity	e	0.0537	m
Arm inertia	I	0.000884	kg·m^2
Spring stiffness	k	170	N/m
Controller parameter	m_c	0.0012	—
Controller parameter	k_c	0.0811	—

TABLE I

PROBLEM DATA FOR THE RTAC SYSTEM.

Description	Manufacturer	Model
Air Bushing	New Way bearings	S301201
Laser sensor	Micro-Epsilon	ILD1300-200
DC motor	MicroMo	3863H012C
Shaft Encoder	MicroMo	HEDM5500J12
Motor Controller	Advanced Motion Controls	12A8
DAQ board	National Instruments	NI6024E
Encoder/Timer	National Instruments	NI 6601

TABLE II

MODEL AND MANUFACTURER INFORMATION OF HARDWARE USED.

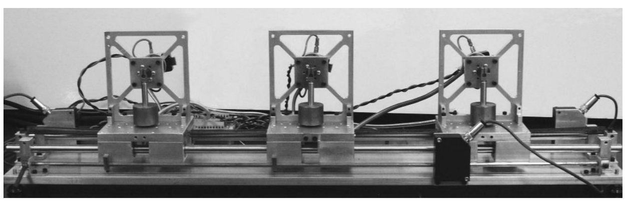

Fig. 1. Multi-RTAC testbed.

IV. HARDWARE DESCRIPTION AND EXPERIMENTAL RESULTS

The experimental testbed constructed to implement the decentralized energy-based hybrid control technique is shown in Figure 1. It consists of an aluminum base with two rails that air bushings float on providing translational motion for the carts with very low friction. Rotary actuators affixed with eccentric arms and masses are fixed to the carts providing the control torques. The actuation is provided by DC motors driven by a set of linear motor controllers, and the measurements of the eccentric arm angles and cart positions are performed with a quadrature encoder on each motor and a laser displacement sensor for each cart, respectively. The controller is implemented with the MathWorks MATLAB®, Simulink®, and xPC Target™ software using National Instruments PCI cards for I/O. The hardware used for the testbed is listed in Table II.

Next, we provide a more detailed description of the experimental testbed. Translational motion for each cart is provided by four air bushings mounted into aluminum blocks. These blocks are mounted to an aluminum plate to form the platforms of the carts. These platforms are also constructed to deliver air to the bushings through internal passageways to eliminate excessive air fittings. The air bushings float on two stainless steel precision shafts of 0.5 in in diameter that are affixed to the aluminum base. Negligible damping effects result from the motor and rail friction, resistance from hoses and wires, and air resistance. Supports are attached to the platforms to facilitate mounting of the rotational actuators and the proof-masses. The supports are designed in such a manner that they can be mounted either vertically or

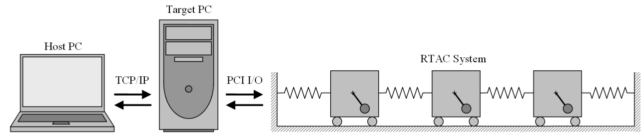

Fig. 2. Diagram of real-time target implementation.

horizontally. This enables the experiment to be carried out with and without gravitational effect on the proof-masses. Four pretensioned extension springs attach the carts to each other and to fixed supports mounted on the base. The springs are easy to remove so that springs with different stiffnesses can be used. The spring stiffness constant used for the testbed was measured to be 170 N/m and the springs are shown to be linear throughout the usable range. The control torque for each cart in the system is provided by means of a proof-mass attached to an actuator by an eccentric arm. The arms are constructed in such a way that various proof-masses may be used. The actuators are 12 volt DC motors which generate a continuous torque of 0.11 N·m each with a stall torque of 1.2 N·m, and have a thermally limited continuous current of 7.6 A. Driving the motors are a set of PWM servo amplifiers which can supply a peak current of 12 A and a continuous current of 6 A. The units are operated in current mode producing currents which are proportional to the input voltages. The motor controllers have built-in current limiters to protect the motors from high torque commands.

Measurement of the system states was accomplished with quadrature encoders and laser displacement sensors. The quadrature encoders measure the angular positions and velocities of the proof-masses. The encoders are attached to the back of the motors and have 1024 line per revolution resolution. This gives an angular resolution of 0.09° when used in quadrature mode. Positions of the translational masses are measured with laser sensors that use optical triangulation to measure displacement while velocities are obtained by numerical differentiation of position data. The sensors measure position with a static resolution of 100 μm and dynamic resolution of 200 μm at a rate of 500 Hz and with a measurement range of 200 mm. Laser sensors were selected over other linear measurement sensors since they do not influence the motion of the carts.

To implement the decentralized energy-based hybrid control in real time the MathWorks MATLAB®, Simulink®, and xPC Target™ software were used. The diagram in Figure 2 illustrates the hardware layout. The control law is created in Simulink®, then compiled into C code, and then downloaded onto the target PC. The target PC runs a real time operating system that executes the Simulink® block diagram. The Input/Output for the target PC consists of National Instruments PCI-6024E and PCI-6601 PCI cards. The PCI-6024E cards are used to acquire the distances measured by the laser sensors, and to send voltages to the motor controllers to generate the required control torques, while the PCI-6601 card is used to read the encoders to obtain the angles and directions of rotation of the proof-masses.

Next, we show experimental results obtained from implementing the decentralized energy-based hybrid control framework presented in Section II on the multi-RTAC testbed. The system parameters are shown in Table I with initial conditions $q_1(0) = -0.074$ m, $q_2(0) = -0.012$ m, $q_3(0) = -0.0055$ m, $\dot{q}_i(0) = 0$, $\theta_i(0) = 0$, $\dot{\theta}_i(0) = 0$, $q_{ci}(0) = 0$, and $\dot{q}_{ci}(0) = 0$, $i = 1, 2, 3$. Figure 3 shows positions of the carts versus time while Figure 4 shows the carts velocities versus time. Figure 5 shows the angular positions of the pendulums versus time and Figure 6 shows

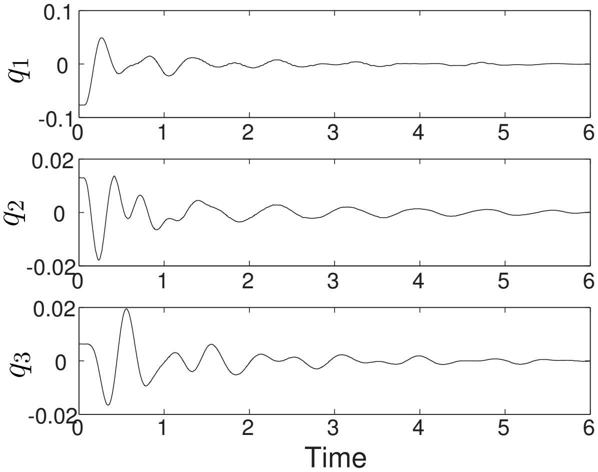

Fig. 3. Positions of the carts in meters versus time.

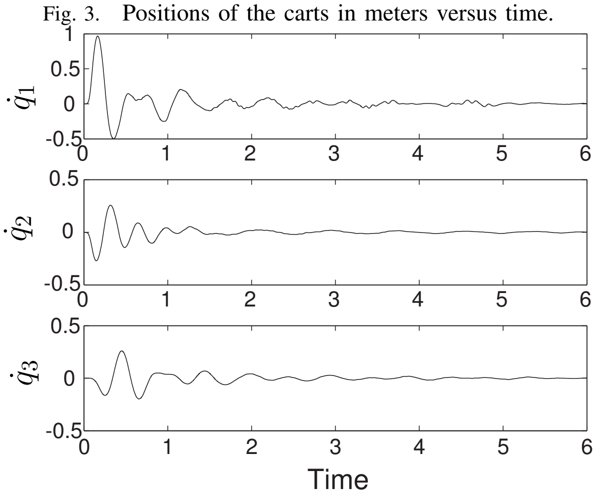

Fig. 4. Velocities of the carts in m/s versus time.

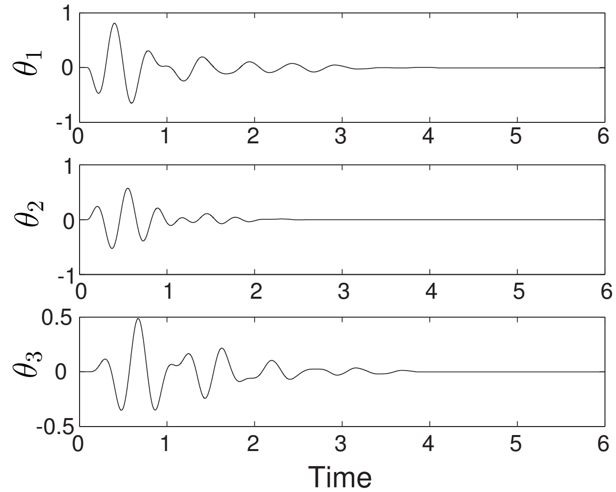

Fig. 5. Angular positions of the pendulums in radians versus time.

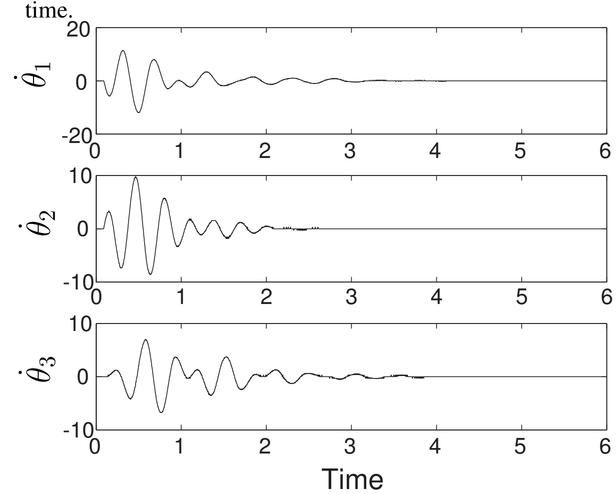

Fig. 6. Angular velocities of the pendulums in rad/sec versus time.

their angular velocities versus time. Figures 7 and 8 show the time history of each subcontroller states. Note that each subcontroller states are discontinuous according to (24). The control torques versus time are shown in Figure 9 and are discontinuous at the resetting times as follows from (24) and (25). Figure 10 shows the physical energy of the plant, combined emulated energy of all subcontrollers, and the total energy of the multi-RTAC system which is the sum of the previous two. Although the sum of the plant energy and controller emulated energy is supposed to remain constant between resettings as shown in (11), in the experimental setup the slight decreases in total energy are the result damping effects that are always present in a physical system.

V. Conclusion

In this paper, we specialize the decentralized energy-based hybrid control framework developed in [9] to stabilization of interconnected Euler-Lagrange dynamical systems. The control technique uses the coupling between the physical dynamical system and controller to efficiently remove real energy from the physical system. Specifically, the states of the dynamic controller reset in such a way that the real plant energy is always dissipated through the motion of the actuators. In other words, the actuators never supply the physical energy back to the system due to controller state resettings. We further implemented this framework in real time on the example of the multi-RTAC system. The experimental data obtained agree with numerical simulations and show the efficacy of the theoretical framework.

References

[1] D. D. Šiljak, *Large-Scale Dynamic Systems: Stability and Structure*. New York, NY: Elsevier North-Holland Inc., 1978.

[2] R. Saeks, "On the decentralized control of interconnected dynamical systems," *IEEE Trans. Autom. Contr.*, vol. 24, pp. 269–271, 1979.

[3] M. E. Sezer and O. Huseyin, "On decentralized stabilization of interconnected systems," *Automatica*, vol. 16, pp. 205–209, 1980.

[4] M. G. Singh, *Decentralised Control*. New York: North-Holland, 1981.

[5] J. Bernussou and A. Titli, *Interconnected Dynamical Systems: Stability, Decomposition, and Decentralisation*. New York: North-Holland, 1982.

[6] M. Jamshidi, *Large-Scale Systems*. New York: North-Holland, 1983.

[7] A. Linnemann, "Decentralized control of dynamically interconnected systems," *IEEE Trans. Autom. Contr.*, vol. 29, pp. 1052–1054, 1984.

[8] J. C. Willems, "Dissipative dynamical systems Part I: General theory," *Arch. Rational Mech. Anal.*, vol. 45, pp. 321–351, 1972.

[9] W. Haddad, Q. Hui, V. Chellaboina, and S. Nersesov, "Hybrid decentralized maximum entropy control for large-scale dynamical systems," *Nonlinear Analysis: Hybrid Systems*, vol. 1, pp. 244–263, 2007.

[10] Y. Kishimoto and D. S. Bernstein, "Thermodynamic modeling of interconnected systems I: Conservative coupling," *J. Sound Vibr.*, vol. 182, pp. 23–58, 1995.

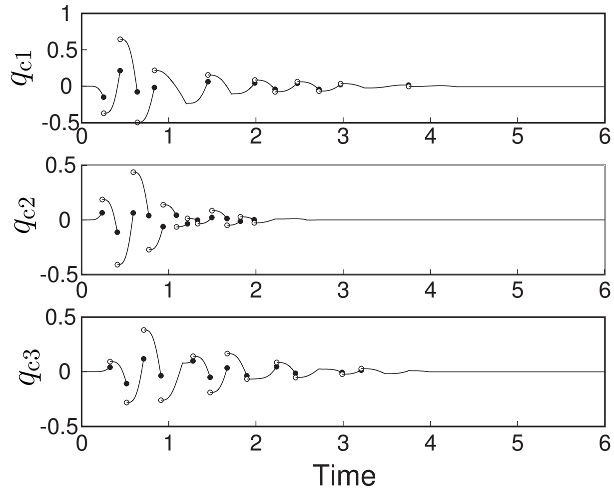

Fig. 7. Subcontroller positions versus time.

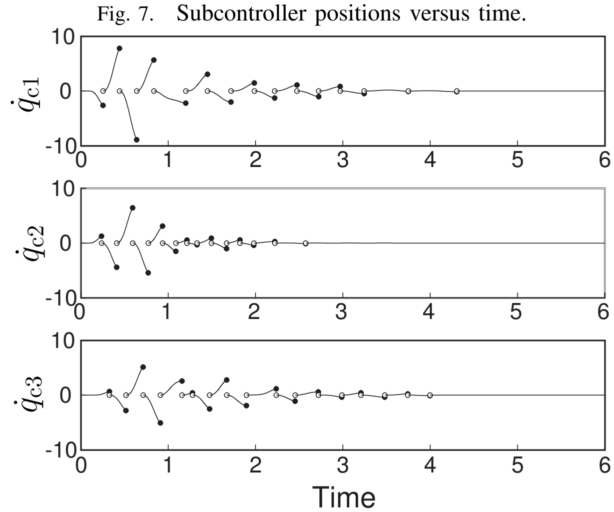

Fig. 8. Subcontroller velocities versus time.

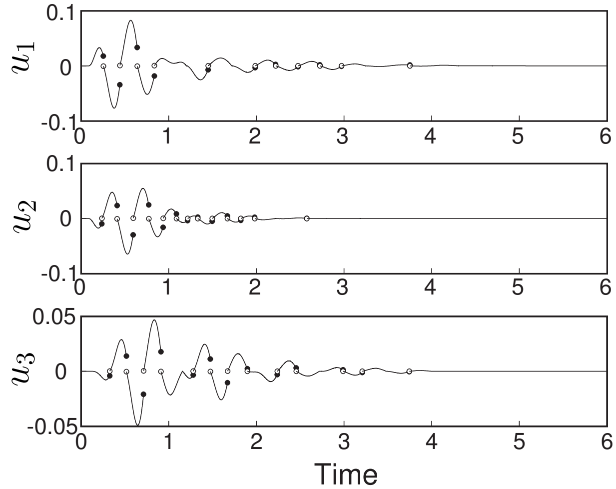

Fig. 9. Control torques in N·m versus time.

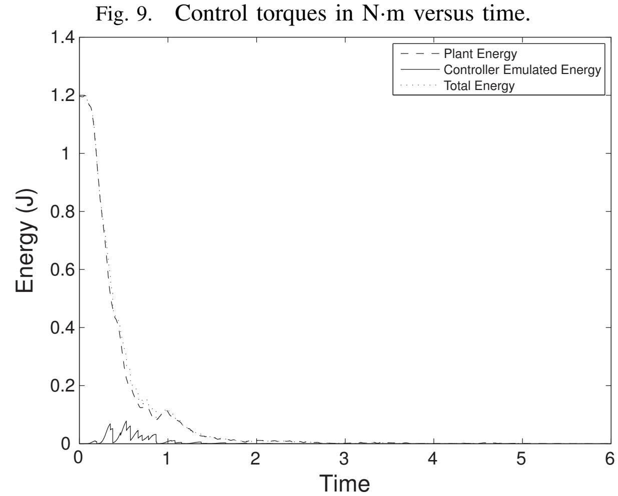

Fig. 10. Plant, combined subcontroller, and total energies versus time.

[11] W. M. Haddad, V. Chellaboina, Q. Hui, and S. G. Nersesov, "Energy- and entropy-based stabilization for lossless dynamical systems via hybrid controllers," *IEEE Trans. Autom. Contr.*, vol. 52, no. 9, pp. 1604–1614, 2007.

[12] V. Lakshmikantham, D. D. Bainov, and P. S. Simeonov, *Theory of Impulsive Differential Equations*. Singapore: World Scientific, 1989.

[13] D. D. Bainov and P. S. Simeonov, *Systems with Impulse Effect: Stability, Theory and Applications*. England: Ellis Horwood Limited, 1989.

[14] W. M. Haddad, V. Chellaboina, and S. G. Nersesov, *Impulsive and Hybrid Dynamical Systems. Stability, Dissipativity, and Control*. Princeton, NJ: Princeton University Press, 2006.

[15] M. Jankovic, D. Fontaine, and P. V. Kokotovic, "TORA example: Cascade- and passivity-based control designs," *IEEE Trans. Contr. Sys. Tech.*, vol. 4, no. 3, pp. 292–297, 1996.

[16] R. T. Bupp, D. S. Bernstein, and V. T. Coppola, "A benchmark problem for nonlinear control design," *Int. J. Robust and Nonlinear Control*, vol. 8, pp. 307–310, 1998.

[17] ——, "Experimental implementation of integrator backstepping and passive nonlinear controllers on the RTAC testbed," *Int. J. Robust and Nonlinear Control*, vol. 8, pp. 435–457, 1998.

[18] R. T. Bupp, D. S. Bernstein, V. Chellaboina, and W. M. Haddad, "Resetting virtual absorbers for vibration control," *J. Vibr. Contr.*, vol. 6, pp. 61–83, 2000.

[19] C.-J. Wan, D. S. Bernstein, and V. T. Coppola, "Global stabilization of the oscillating eccentric motor," *Nonlinear Dynamics*, vol. 10, pp. 49–62, 1996.

[20] M. Antonio and W. Yu, "Nonlinear benchmark system identification with partial states measurement," in *Proc. IEEE Conf. Dec. Contr.*, Phoenix, AZ, 1999, pp. 1077–1082.

[21] J. M. Avis, S. G. Nersesov, and R. Nathan, "Energy-based hybrid control for the RTAC system: Experimental results," in *Proc. Amer. Contr. Conf.*, Seattle, WA, 2008, pp. 3331–3336.

[22] H. Poincaré, "Sur le probléme des trois corps et les équations de la dynamique," *Acta Math.*, vol. 13, pp. 1–270, 1890.

[23] W. M. Haddad, V. Chellaboina, and S. G. Nersesov, "Time-reversal symmetry, Poincaré recurrence, irreversibility, and the entropic arrow of time: From mechanics to system thermodynamics," *Nonlinear Analysis: Real World Applications*, vol. 9, pp. 250–271, 2008.

[24] A. Pikovsky, M. Rosenblum, and J. Kurths, *Synchronization: A Universal Concept in Nonlinear Sciences*. Cambridge, UK: Cambridge University Press, 2003.

[25] H. Nijmeijer and A. Rodriguez-Angeles, *Synchronization of Mechanical Systems*. Singapore: World Scientific, 2003.

[26] G. V. Osipov, J. Kurths, and C. Zhou, *Synchronization in Oscillatory Networks*. Berlin: Springer, 2007.

[27] S. H. Strogatz, *Nonlinear Dynamics and Chaos: With Applications to Physics, Biology, Chemistry and Engineering*. Cambridge, MA: Perseus Books, 1994.